References

1. Yamazaki, I.; Tamai, N.; Yamazaki, T. *J. Phys. Chem.* **1990**, *94*, 516.
2. (a) Stryer, L. *Ann. Rev. Biochem.* **1978**, *47*, 819. (b) Kim, H.; Kang, T. J. *J. Photoscience* **1994**, *1*, 75.
3. Bradley, D. D. C.; Brown, A. R.; Burns, P. L.; Burroughes, J. H.; Friend, R. H.; Holmes, A. B.; Mackay, K. D.; Marks, R. N. *Synthetic Metals* **1991**, *41-43*, 3135.
4. Kasha, M. *Disc. Faraday Soc.* **1950**, *9*, 14.
5. Birks, J. B. *The Theory and Practice of Scintillation Counting*; Pergamon: Oxford, 1964.
6. (a) Birks, J. B. In *Organic Scintillators and Liquid Scintillation Counting*; Horrocks, D. L.; Peng, C. T., Eds; Academic Press: New York, 1971; p 3. (b) Horrocks, D. L. *Applications of Liquid Scintillation Counting*; Academic Press: 1974. chapter 1.
7. Renschler, C. L.; Harrah, L. A. *Nucl. Instr. Meth. in Phys. Res.* **1985**, *A235*, 41.
8. (a) Kirkbright, G. F.; Narayanqswarmy, R.; West, T. S. *Anal. Chem. Acta* **1970**, *52*, 237. (b) Catalan, J. *J. Am. Chem. Soc.* **1990**, *112*, 747.
9. (a) Chou, P.; Aartsma, T. J. *J. Phys. Chem.* **1986**, *90*, 721. (b) Parthenopoulos, D. A.; McMorrow, D.; Kasha, M. *J. Phys. Chem.* **1991**, *95*, 2668.
10. D'ambrosio, C.; Leutz, H.; Taufer, M.; Güsten, H. *Appl. Spectroscopy*, **1991**, *45*, 484.
11. (a) Frey, W.; Laermer, F.; Elsaesser, T. *J. Phys. Chem.* **1991**, *95*, 10391. (b) Laermer, F.; Elsaesser, T.; Kaiser, W. *Chem. Phys. Lett.* **1988**, *148*, 119.
12. Bross, A. D.; Pla-Dalmau A.; Spangler, C. W. *Radiat. Phys. Chem.* **1993**, *41*, 379.
13. Drexhage, K. H.; In *Standardization in Spectrophotometry and Luminescence Measurements, National Bureau of Standards Special Publication 466*; Mielenz, K. D.; Velapoldi, R. A.; Mavrodineanu, R. Eds. 1975; p 33.
14. (a) Becker, R. S.; Lenoble, C.; Zein, A. *J. Phys. Chem.* **1987**, *91*, 3509. (b) Itoh, M.; Fujiwara, Y. *J. Am. Chem. Soc.* **1985**, *107*, 1561.
15. (a) Förster, Th. *Z. Naturforsch. A*, **1949**, *4*, 321. (b) Förster, Th. *Disc. Faraday Soc.* **1959**, *27*, 7.
16. Cohen, S. G.; Weinreb, A. *Proc. Phys. Soc. LXIX*, **1956**, 593.
17. Berlman, I. B. *J. Chem. Phys.* **1960**, *33*, 1124.
18. (a) Basile, L. J. *J. Chem. Phys.* **1962**, *36*, 2204. (b) Vala Jr., M. T.; Haebig, J.; Rice, S. A. *J. Chem. Phys.* **1965**, *43*, 886.
19. Berman, H. A.; Yguerabide, J.; Taylor, P. *Biochemistry* **1980**, *19*, 2226.
20. (a) Torikai, A. In *Handbook of Polymer Science and Technology*; Cheremisinoff, N. P., Ed.; Marcel Dekker Inc: New York, 1989; Vol. 1, p 605. (b) Tanigaki, K.; Tateishi, K.; ibid, p 307.
21. Torikai, A.; Kato, S.; Fueki, K. *Polym. Degrad. Stab.* **1987**, *17*, 21.
22. Brewer, W. E.; Martinez, M. L.; Chou, P.-T. *J. Phys. Chem.* **1990**, *94*, 1915.

The Oxide Coating Effects on the Magnetic Properties of Amorphous Alloys

Young Je Bae, Ho G. Jang†, and Hee K. Chae*

Department of Chemistry, Hankuk University of Foreign Studies, Yongin 449-791, Korea
†Department of Chemistry, Korea University, Seoul 136-701, Korea

Received March 9, 1996

A variety of metal oxides were coated by sol-gel process from their metal alkoxides on the ribbons of Co-based and Fe-based amorphous alloys, and the effects of surface oxide coating on the magnetic properties of the alloy are investigated. The core loss is found to be reduced significantly by the oxide coating, the loss reduction becoming more prominent at higher frequencies. The shape of the hystersis loop is also dependent upon the kind of the coated metal oxide. The coatings of MgO, SiO_2, $MgO \cdot SiO_2$ and $MgO \cdot Al_2O_3$ induce tensile stress into the Fe-based ribbon whereas those of BaO, Al_2O_3, $CaO \cdot Al_2O_3$, $SrO \cdot Al_2O_3$ and $BaO \cdot Al_2O_3$ induce compressive stress. These results may be explained by the modification of domain structures *via* magnetoelastic interactions with the shrinkage stress induced by the sol-gel coating.

Introduction

Interest in the sol-gel process of inorganic oxide materials began as early as the mid-1800s with Ebelman and Graham's studies on silica gels.[1] Since then, the sol-gel process has been developed to prepare thin films, monoliths, fibers and monosized powders of metal oxides.[1~3] It has some potential profits for good homogeneity, ease of chemical composition control, high purity, low temperature processing, and large area and versatile shaping over vacuum deposition techni-

ques. Thin films (normally <1 μm in thickness) formed by dipping or spinning benefit from most of the advantages of the sol-gel process and are one of the few successful commercial applications. Since the early applications for sol-gel films were optical coatings,[4] many new uses for sol-gel films or coatings have appeared in electronics, protection, membrane and sensor applications.[1,2]

Here we can extend the sol-gel process to the fabrication of coatings on magnetic materials, especially amorphous alloy ribbons that exhit excellent soft magnetic properties and are currently used in electromagnetic switching devices at high frequencies. Since the core loss (W_L) increases exponentially with the frequency, it becomes quite large at hundreds kHz, and increases the temperature of the core itself and neighboring parts deteriorating the performance of them. The most common way of reducing the core loss at high frequencies is to coat an insulating layer on ribbon surface so that eddy currents can be confined within the ribbon. A conventional coating method is to dip a ribbon into the mixture of fine oxide powders in water or organic solvents.[5~7] This method, however, has some difficulties to control the thickness and uniformity of oxide films as soon as it applies to thinner ribbon-type magnetic materials.

In this paper, we applied the sol-gel process to coat various metal oxide layers on the ribbons of a Co-based amorphous alloy and an Fe-based amorphous alloy, and investigated the effects of the oxide coating on the magnetic properties of the amorphous alloys.

Experimental

Materials and Metal Alkoxides. The ribbons of amorphous alloys, the Co-based 2714A($Co_{66}Fe_4NiB_{14}Si_{15}$) with zero magnetostriction and Fe-based 2605S3A($Fe_{76.5}Cr_2B_{16}Si_5C_{0.5}$) with the saturation magnetostriction of 20 ppm were supplied by AlliedSignal Co., USA. The width and thickness of the ribbons are 4.48 mm and ca 20 μm, respectively. The synthesis of metal alkoxide precursors is described in detail elsewhere.[8] The solution of magnesium methoxyethoxide [$Mg(OCH_2CH_2OCH_3)_2$] for MgO coating was prepared by reaction of excess (8 mol) 2-methoxyethanol ($CH_3OCH_3CH_3OH$, Aldrich) with one mole of magnesium ethoxide [$Mg(OCH_2CH_3)_2$, Aldrich]. Similarly, the other precursor solutions for single metal oxides were prepared by the exchange reaction of metal alkoxides with excess 2-methoxyethanol. For bimetallic precursors, a solution of one metal alkoxide was added equivalently to a solution of the other metal alkoxide, and the mixed solutions were then refluxed. Hydrolysis was carried out by adding a solution of water and alcohol to the precursor.

Film Preparation. A variety of metal oxides which were coated on the amorphous alloy ribbons by sol-gel dipping process are shown in Scheme 1: MgO, BaO, Al_2O_3, SiO_2, $MgO\cdot Al_2O_3$, $SrO\cdot Al_2O_3$, $BaO\cdot Al_2O_3$, and $MgO\cdot SiO_2$. The reasonable thickness (μm) of the coated layer can be adjusted by the concentrations of metal alkoxides and water in the precursor solution. The speed of dipping the alloy ribbon into the precursor solution was 4.33 cm/sec. After dipping, the ribbon was dried at 200 ℃. It is noted here that all the coating procedures were carried out in a dry nitrogen atmosphere.

Table 1. The results for the average thickness of the coated oxides on the Fe-based ribbon

Types of oxide layer	Precursor solution in 2-methoxyethanol	Concentration of metal alkoxide (M)	Average thickness of coated layer (μm)
MgO	$Mg(OCH_2CH_2OCH_3)_2$	0.5	0.70
BaO	$Ba(OCH_2CH_2OCH_3)_2$	0.5	0.40
Al_2O_3	$Al_2(OCH_2CH_2OCH_3)_3$	0.5	0.39
SiO_2	$Si(OCH_2CH_2OCH_3)_4$	0.5	0.65
$MgO\cdot Al_2O_3$	$MgAl_2(OCH_2CH_2OCH_3)_8$	0.5	0.75
$CaO\cdot Al_2O_3$	$CaAl_2(OCH_2CH_2OCH_3)_8$	0.5	1.92
$SrO\cdot Al_2O_3$	$SrAl_2(OCH_2CH_2OCH_3)_8$	0.5	1.68
$BaO\cdot Al_2O_3$	$BaAl_2(OCH_2CH_2OCH_3)_8$	0.5	1.80
$MgO\cdot SiO_2$	$MgSi(OCH_2CH_2OCH_3)_6$	0.5	1.39

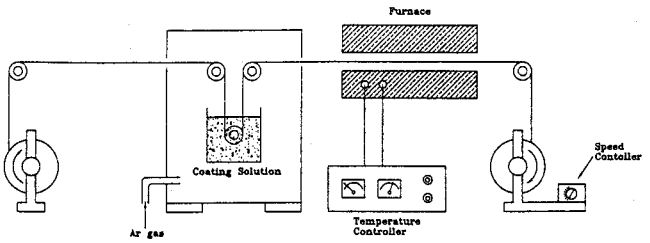

Scheme 1. Schematic diagram of sol-gel dip coating process, showing the sequential stages of dipping and drying at 200 ℃.

Measurements of Magnetic Propeties. The thickness of a coated layer was measured by using a digital micrometer. In order to increase the accuracy of the measurement, a stack consisting of about 10-20 ribbons was first measured and the thickness of each ribbon was then obtained by dividing the total stack thickness by the number of ribbons in the stack. The winding tension was hand tight. The results for the average thickness of coated oxide layer are reported in Table 1. The measured thickness ranges from 0.39 to 1.92 μm. It is worth noting that the thickness of single oxides is generally much smaller than that of oxide mixtures.

The ribbons were wound onto toroidal cores with inner diameter of 19 mm. The cores were annealed at 400 ℃ for 30 min or 1 hr for the Co-based ribbon and at 435 ℃ for 2 hr for the Fe-based ribbon under N_2 gas atmosphere, and then air-cooled. The dc magnetic properties were measured with a hysteresis loop tracer. The core loss (W_L) was measured by using a B-H analyzer (Iwatsu Co. Model No. SY-8216) at frequencies up to 500 kHz with magnetic flux densities of 0.1, 0.2, 0.3 and 0.4 T for the Co-based ribbon, and up to 200 kHz with magnetic flux densities of 0.1, 0.3, 0.5, 0.7 and 1.0 T for the Fe-based ribbon.

Results and Discussion

In the case of the Co-based ribbon, Figure 1 shows the results for core loss (W_L, watts/kg) at 200 kHz and 0.3 T as a function of thickness (t) of the oxide coated film. The values of W_L for the samples annealed for 1 hr (indicated

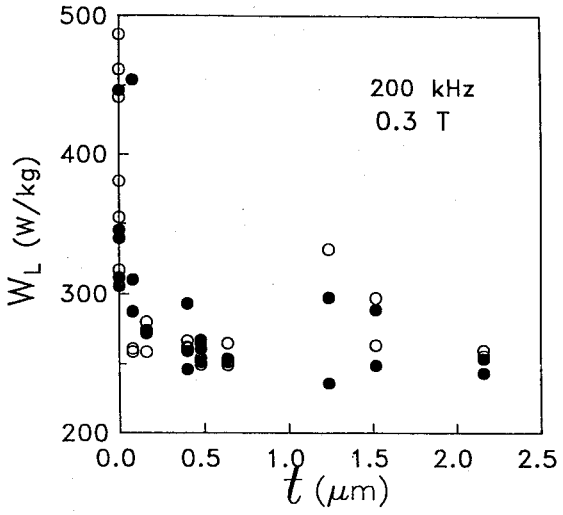

Figure 1. The value of WL of the Co-based ribbon at 200 kHz and 0.3 T as a function of oxide thickness (t). The results for the sample heat-treated for 1 hr at 400 ℃ are indicated by filled circles and those for the sample heat-treated for 30 min are indicated by open circles.

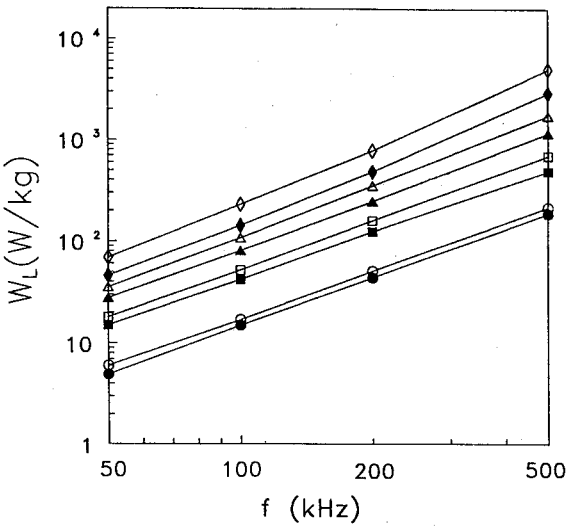

Figure 2. The value of W_L of the Co-based ribbon as a function of frequency (f). The results measured at B=0.1, 0.2, 0.3 and 0.4 T are indicated by circles, squares, triangles and diamonds, respectively. The uncoated and coated samples are indicated by open and filled symbols, respectively.

by filled circles) and 30 min (indicated by open circles) are similar to each other. The value of W_L decreases rather significantly with t until $t \simeq 0.4$ μm and then remains nearly constant with t. The loss reduction with t becomes more prominent as frequency (f) increases, indicating the importance of the effect of coating at high frequencies. It is interesting to note that the scattering in the measured values of W_L is very large when the ribbon is not coated or coated only slightly ($t \leq \sim 0.1$ μm), but the data scattering becomes smaller at higher values of t except for $t \simeq 1.25$ μm. This result may be explained as follows. Even uncoated ribbon is considered to have an oxide layer on the surface formed during melt-quenching, but the oxide layer is so thin (~100 Å) that it may not provide a complete insulation between the ribbon layers. As the thickness of the film is over 1 μm, the insulation may be affected by the winding tension or the defect of the film. Generally the thin layer by sol-gel process may be cracked over $t \simeq 1$ μm. The reason for a large data scattering, however, is not understood presently.

Figure 2 shows the results for W_L of the Co-based ribbon as a function of f at fixed values of B=0.1, 0.2, 0.3 and 0.4 T. At each B, the results for uncoated ribbons (indicated by open symbols) and coated ribbons with $t=0.40$ μm (indicated by filled symbols) are shown. A well-known linear relationship between the two values is observed to exist in the log-log plot, except for the results at the high flux density of B=0.4 T where the values of W_L at high f are deviated upward from the linearity. The values of W_L for coated ribbons are lower than those for uncoated ones in the whole frequency range and at all the measured flux densities, as expected. The difference in W_L between uncoated and coated ribbons increases with B, indicating that the need for an insulation coating increases as the operating magnetic flux density increases.

Since the Co-based ribbon was zero magnetostriction, the stress effect was considered to be mainly elastic. It is expected that, if the coating is made on a ribbon with large magnetostriction, the effect of the coating on the magnetic properties are considered to be even more pronounced. It is therefore of interest to investigate the effects of surface coating on the magnetic properties of an Fe-based amorphous alloy with large magnetostriction. The dc magnetic properties of the Fe-based amorphous ribbon coated with a variety of metal oxides are measured and the results are summarized in Table 2. The results for the hysteresis graph itself are also shown in Figure 3(a)-(e) for some typical cases, *viz.*, for the uncoated ribbon and the ribbons coated with MgO, $MgO \cdot Al_2O_3$, BaO, $BaO \cdot Al_2O_3$, respectively. The values of coercive force (H_c) given in Table 2 were obtained by applying the maximum field of 1 Oe. A very large difference in the dc magnetic properties is observed, which is most vividly represented by the shape of the hysteresis graphs. The hysteresis loops for the ribbons coated with MgO, SiO_2, $MgO \cdot SiO_2$ and $MgO \cdot Al_2O_3$ are square-shaped (more squared than

Table 2. The dc magnetic properties of the uncoated ribbon and the ribbons coated with the oxides

Type of coated oxide	μ_i	μ_m	B_r/B_{10}	H_c (mOe)
uncoated	20766	44761	0.4021	67.13
MgO	9425	66364	0.7429	80.00
BaO	12176	14773	0.2012	82.50
Al_2O_3	27679	38808	0.3380	51.25
SiO_2	18902	50506	0.5662	88.75
$MgO \cdot Al_2O_3$	10318	77692	0.7115	90.00
$CaO \cdot Al_2O_3$	23344	29679	0.3421	85.00
$SrO \cdot Al_2O_3$	10000	12383	0.1571	68.75
$BaO \cdot Al_2O_3$	8603	11268	0.1674	80.00
$MgO \cdot SiO_2$	15368	48991	0.4951	68.75

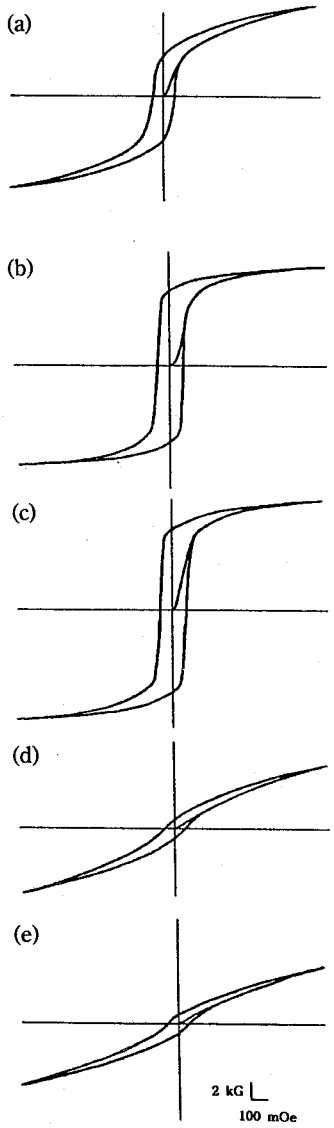

Figure 3. The dc hysteresis loops of the Fe-based ribbon: (a) the uncoated ribbon and the ribbons coated with (b) MgO, (c) $MgO \cdot Al_2O_3$, (d) BaO, (e) $BaO \cdot Al_2O_3$.

uncoated ribbon) with a large value of remnant magnetic flux(B_r)/maximum magnetic flux(B_{10}) and maximum permeabrbility (μ_m) but a small value of initial permearbility (μ_i). The squared-shape (and hence large B_r/B_{10}) may be related to the fact that more domains are aligned in the same direction of applied magnetic field H.[9] The low value of μ_i may be related to low domain density, since magnetization by domain wall movement and domain wall bending is expected to be small when domain density is small. From this, the ribbons coated with these metal oxides are considered to have a large proportion of the domains aligned in the same direction of H. The shape of the hysteresis graphs for the ribbons coated with BaO, Al_2O_3, $CaO \cdot Al_2O_3$, $SrO \cdot Al_2O_3$ and $BaO \cdot Al_2O_3$ is very much inclined with a small value of B_r/B_{10}. The values of μ_m and μ_i are small as is well expected. Here it is important to note that the difference in the values between μ_m and μ_i is small for these ribbons. These dc results may indicate that more domains are aligned in the transverse direction of H. Detailed information on the domain density cannot be drawn from the present dc results, but domains of these ribbons are considered to be more refined than for the ribbons with squared hysteresis loops from the geometrical consideration, among other things, since large domain width result in a very large magnetostatic energy when domains are aligned in the transverse direction. In some cases, the value of coercive force is increased appreciably by the oxide coating with the exception of the Al_2O_3 coating.

The present results indicate that the surface oxide coating not only provides an insulation between the layers but also modifies the domain structure. The core loss due to eddy currents, which constitutes the major component of the total loss at high frequencies, may be divided into the classical eddy current loss due to macroscopic eddy currents and the anomalous loss due to microscopic eddy currents.[10] Macroscopic eddy currents induced from homogeneous magnetization are originally attempted to reduce by confining eddy currents within each layer with the help of the insulation coating. Microscopic eddy currents are induced from the dynamic movement of domain walls, and are proportional to the wall velocity. Since the wall velocity is proportional to the domain wall width under the assumption that all walls are mobile, the anomalous loss is reduced by the domain refinement. The core loss reduction achieved in the present work is considered to result from the decrease in both the macroscopic and the microscopic eddy currents, although the relative importance of the two is not known presently.

It would be also of interest to consider the reason behind the large change in the magnetic properties by the surface coating. The main reason is considered to result from the magnetoelastic effect which is caused by coupling magnetostriction to the stress induced by the sol-gel coating. In the sol-gel process, the most obvious physical change that occurs when the pore liquid is removed by thermal evaporation (drying) is "shrinkage" with weight loss. The shrinkage is dependent upon the kind of metal alkoxide, the existence of the catalyst and the reaction condition, and generally brings a compressive stress on the substrate. But Brinker and Scherer show that it is indeed the difference in shrinkage rate between inside and outside of a drying body that results in a tensile drying stress.[1] According to Dwivedi, the gel shrinkage was primarily perpendicular to the surface at dried thickness less than 80 μm and it was both radial and perpendicular at thickness more than 80 μm.[11] There are therefore two kinds of stresses on the substrate that can exist during the drying stage: tensile or compressive. Since the present Fe-based amorphous alloy has positive saturation magnetostriction (whose value is relatively high being 20 ppm), tensile stress in the horizontal direction of H causes to align domains in the same direction of H, thus resulting in a square-shaped hysteresis loop with a high value of B_r/B_{10}.[12] Similarly, compressive stress leads to an inclined hysteresis graph with a low value of B_r/B_{10}. The tensile stress of the Fe-based ribbon, however, can be modified by the effect of the sol-gel coating. It may be reduced by compressive stress of the oxide layer or increased by tensile stress of the oxide layer when the pore liquid evaporates in the oxide film. It is therefore considered that the coatings of BaO, Al_2O_3, $CaO \cdot Al_2O_3$, $SrO \cdot Al_2O_3$ and $BaO \cdot Al_2O_3$ induce compressive stress. The

other oxides seem to induce some amount of tensile stress.

The induced stresses with physical properties which are obtained depending on the type of coated oxides may be of practical importance. The effects of coatings on the magnetic properties play a similar role to those of magnetic field and/or stress annealing on the magnetic properties. Considering that the formation of induced anisotropy in the transverse direction by magnetic field annealing is known to be not easy and the resulting induced anisotropy energy is small in the case of Fe-based amorphous alloy,[13] the inclination of the hysteresis loop by the sol-gel coating is particularly important. In applications such as choke cores of switching-mode power supply devices, constant permeability over a wide applied field is an important property, which may be achieved by inducing anisotropy in the transverse direction. A rough estimate shows that the energy of induced anisotropy achieved by the present sol-gel coating is about 100 J/m^3. A magnetic field annealing of coated ribbons in the transverse direction is expected to increase the induced anisotropy energy further. Work in this direction is under way and will be published elsewhere.

Acknowledgment. We gratefully acknowledge the support of the fund from the Department of Education, Basic Science Research Institute Program under contract BSRI-95-3407 and are very grateful to Dr. Sang Ho Lim and Mr. Yong Seok Choi of Korea Institute of Science and Technology for many helpful discussions.

References

1. Brinker, C. J.; Scherer, G. W. *Sol-Gel Science: The Physics and Chemistry of Sol-Gel Processing*; Academic Press: New York, 1990.
2. Klein, L. C., Ed. *Sol-Gel Technology for Thin Films, Fibers, Preforms, Electronics, and Specialty Shapes*; Noyes Publications: Park Ridge, NJ, 1988.
3. Brinker, C. J.; Clark, D. E.; Ulrich, D. R., Eds. *Better Ceramics Through Chemistry*; Material Research Society: Pittsburgh, PA, 1984; vol. 32.
4. Hass, G., Ed. *Physics of Thin Films*; Academic Press: New York, 1969, pp 87-141.
5. Nathasingh, D. M.; Smith, C. H.; Datta, A. *IEEE Trans. Magn.* **1984**, *20*, 1332.
6. Thornburg, D. R.; Swift, W. M. *IEEE Trans. Magn.* **1979**, *15*, 1592.
7. Inokuti, Y.; Suzuki, K.; Kobayashi, Y. *J. Japan Inst. Metals* **1995**, *59*, 213.
8. Bradley, D. C.; Mehrotra, R. C.; Gaur, D. P. *Metal Alkoxide*; Academic Press: London, 1978.
9. Chikazumi, S. *Physics of Magnetism*; John Wiley & Sons: New York, 1964, chap. 12.
10. Pfutner, H.; Schonhuber, P.; Erbil, B.; Harasko, G. *IEEE Trans. Magn.* **1991**, *27*, 3426.
11. Dwivedi, R. K. *J. Mater. Sci. Lett.* **1986**, *5*, 373.
12. Cullity, B. D. *Introduction to Magnetic Materials*; Addison-Wesley: Reading, 1972; chap. 12.
13. Liebermann, H. H., Ed. *Rapidly Solidified Alloys*; Marcel Dekka: New York, 1993; chap. 17.

Catalytic Oxygenation of Alkenes and Alkanes by Oxygen Donors Catalyzed by Cobalt-Substituted Polyoxotungstate

Wonwoo Nam*, Sook Jung Yang, and Hyungrok Kim†

Department of Chemistry, Ewha Womans University, Seoul 120-750, Korea
†Catalytic Research Division, Korea Research Institute of Chemical Technology, Taejon 305-606, Korea
Received March 9, 1996

The cobalt-substituted polyoxotungstate [$(CoPW_{11}O_{39})^{5-}$] has been used as a catalyst in olefin epoxidation and alkane hydroxylation reactions. The epoxidation of olefins by iodosylbenzene in CH_3CN yielded epoxides predominantly with trace amounts of allylic oxidation products. *cis*-Stilbene was streoselectively oxidized to *cis*-stilbene oxide with small amounts of *trans*-stilbene oxide and benzaldehyde formation. The epoxidation of carbamazepine (CBZ) by potassium monopersulfate in aqueous solution gave the corresponding CBZ 10,11-oxide product. Other transition metal-substituted polyoxotungstates (M=Mn^{2+}, Fe^{2+}, Ni^{2+}, and Cu^{2+}) were inactive in the CBZ epoxidation reaction. The cobalt-substituted polyoxotungstate also catalyzed the oxidation of alkanes with *m*-chloroperbenzoic acid to give the corresponding alcohols and ketones. The presence of CH_2Br_2 in the hydroxylation of cyclohexane afforded the formation of bromocyclohexane, suggesting the participation of cyclohexyl radical. In the ^{18}O-labeled water experiment, there was no incorporation of ^{18}O into the cyclohexanol product when the hydroxylation of cyclohexane by MCPBA was carried out in the presence of $H_2{}^{18}O$. Some mechanistic aspects are discussed as well.

Introduction

The controlled and selective oxidation of hydrocarbons under mild conditions has been a tantalizing challenge for chemists to develop new technologies for industrial applications.[1] Often-used catalysts for the oxidation reactions are transition